

## Diffusion weighted MR nerve sheath imaging (DW-NSI) using diffusion-sensitized driven-equilibrium (DSDE)

M. Obara<sup>1</sup>, T. Takahara<sup>2</sup>, M. Honda<sup>3</sup>, T. Kwee<sup>4</sup>, Y. Imai<sup>3</sup>, and M. Van Cauteren<sup>1</sup>

<sup>1</sup>Healthcare, Philips Electronics Japan, Minato-ku, Tokyo, Japan, <sup>2</sup>Department of Biomedical Engineering, Tokai University School of Engineering, Hiratsuka, Kanagawa, Japan, <sup>3</sup>Department of Radiology, Tokai University Hospital, Isehara, Kanagawa, Japan, <sup>4</sup>University Medical Center Utrecht, Utrecht, Netherlands

**INTRODUCTION:** The use of diffusion-weighted imaging (DWI) for the evaluation of peripheral nerves was recently introduced by Takahara et al. [1]. Since the signal from the nerves at DWI originates from water within the nerve sheath, this method can be referred to as diffusion-weighted nerve sheath imaging (DW-NSI). There are two major limitations related to echo-planar imaging (EPI)-based DW-NSI: 1) anatomical position shift due to B0 inhomogeneity, and 2) signal discontinuity or inhomogeneity due to axial slice acquisition even though coronally reformatted images are used for reading. The reasons for axial-based acquisition are severe susceptibility and B0 inhomogeneity effects on direct coronal images. The so-called “diffusion-prepared” sequence, also known as driven-equilibrium (DE) Fourier transform (DEFT), was proposed in the early 1990s [2,3]. Since it does not employ EPI but gradient-echo readout, image distortion can largely be prevented making direct coronal imaging feasible. Recently, this preparation concept has been applied for blood signal suppression using smaller sensitizing gradients, which is called motion-sensitized driven-equilibrium (MSDE) [4,5], and several optimizations were proposed [6,7]. The purposes of this study were to assess the utility of the latest MSDE preparation design but with larger sensitizing gradients for DW-NSI, and to compare this new approach to the conventional EPI approach for DW-NSI, at 3.0T. In line with the name MSDE, we called the proposed DEFT technique “diffusion-sensitized driven-equilibrium” (DSDE).

**METHODS:** Five healthy adult subjects (mean age: 29 years) were scanned at 3.0T (Philips Achieva R3). DW-NSI was acquired using a DSDE combined sequence from the C1 nerve to the T1 nerve. Design of the DSDE sequence was similar to that of the latest MSDE [6,7], but with larger sensitizing gradients. Since it can be assumed that DSDE is naturally very sensitive to motion effects because of using diffusion-sensitizing gradients, two kinds of DSDE pulse designs were implemented here: one is the standard design (Conv-DSDE) [6,7] shown in Fig. 1a and another is that gradients sequence was designed for motion compensation (MC-DSDE) shown in Fig. 1b [8]. Adiabatic refocusing pulses [9] and additional gradients inserted in front of the sequence [10] were used to reduce B0 and B1 inhomogeneity, and eddy current effects. Data acquisition using segmented gradient echo (Turbo field echo: TFE) was performed immediately after DSDE preparation. To eliminate T1 effects in acquired signal by TFE, phase cycling scheme was used [2,3]. Conv-DSDE and MC-DSDE sequences were compared to each other and to conventional axial based EPI-DWI. **Acquisition parameters for DSDE:** TR/TE (or echo space) 4.4/2.1ms; FA 10°; ETL 30; STIR fat suppression, inserted before DSDE preparation with 235ms interval; b-factor 400s/mm<sup>2</sup>; 3D slab thickness 92mm; voxel size 2.1\*2.1\*4.0mm (23 partitions); NEX 1(\*2 phase cycling); SENSE factor 2.0, acquisition time 7m08s. **Acquisition parameters for EPI-DWI:** TR/TE 10000.0/90.0ms; FA 90°; ETL 89; half-Fourier factor 0.889; STIR fat suppression with 250ms delay time; b-factor 800 s/mm<sup>2</sup>; NEX 5; SENSE factor 2.0, acquisition time = 4m00s. Other geometry-related parameters were the same as those used for the DSDE acquisitions. The continuity of the spinal cord was evaluated using a three-point grading scale (2=spinal cord is visualized continuously; 1=spinal cord is visualized not continuously with low intensity signal areas; 0=a part of the spinal cord is not visualized, resulting in discontinuity). The distortion of the spinal cord was measured as the positional shift of the spinal cord at EPI-DWI and DSDE relative to that at the anatomical image (survey scan) at 5cm above and below the center of the image. Clinical image quality of the nerves was evaluated by consensus of two board-certified radiologists using a five-point grading scale (4=the nerve is visualized more than 2 cm in length from the peripheral edge of the ganglion homogeneously; 3=the nerve is visualized more than 2 cm in length from the peripheral edge of the ganglion but a part of the nerve is inhomogeneous; 2=the nerve is visualized less than 2cm but more than 1cm; 1=the nerve is visualized less than 1cm; 0=the nerve is not visualized) at all levels from C1 to T1.

**RESULTS:** Representative images are shown in Fig. 2. The image with MC-DSDE is apparently superior to the other images with less distortion, more smoothness, and without jaggy effects as seen on axial EPI-DWI (a). The continuity of the spinal cord was graded as 0.40±0.55 on Conv-DSDE and all were scored as 2.0 on EPI-DWI and MC-DSDE. Distortion was less on MC-DSDE than on EPI-DWI in both the upper and lower parts of the image (5.98±5.63mm vs. 17.02±7.88mm, and 2.88±1.57mm vs. 4.64±1.44mm). Clinical image quality of MC-DSDE was superior to EPI-DWI (18.90±3.21 vs 15.30±2.50). Conv-DSDE was excluded from the last two comparisons because of its poorest score regarding the continuity of spinal cord.

**CONCLUSION:** Our results show that MC-DSDE is an appropriate method for nerve sheath imaging because it offers good signal continuity and less distortion. Further clinical assessment is needed to evaluate its ability to detect and differentiate lesions in the peripheral nervous system.

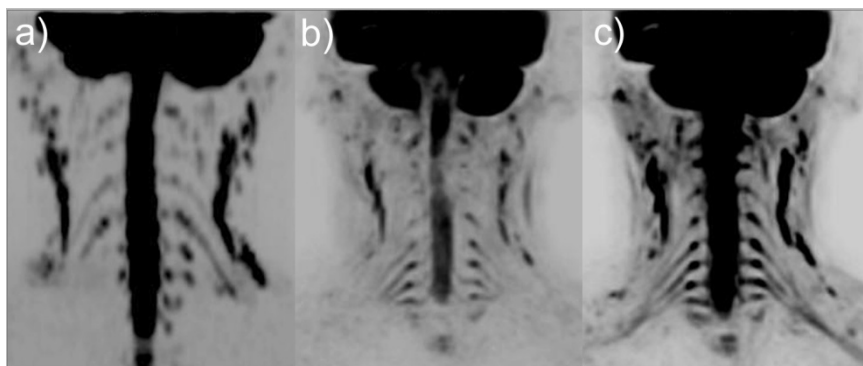


Fig. 2 Coronal reformatted MIP image by EPI-DWI (a), Conv-DSDE (b) and MC-DSDE (c).

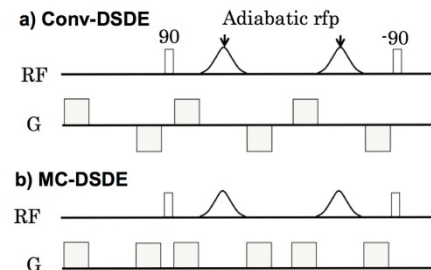


Fig. 1: Two DSDE preparation schemes

## REFERENCES

1. Takahara T et al. Radiology 2008;249:653-60
2. Coremans J et al, JMR 1997;124:323-342
3. Thomas DL et al, MRM 1998;39:950-960
4. Koktzoglou I et al, JMRI 2007;25:815-823
5. Wang J et al, MRM 2007;58:973-981
6. Obara M et al, Proc. ISMRM 2009;p.4547
7. Wang J et al, JMRI 2010; 31:1256-1263
8. Dou J et al, MRM 2002;48:105-114
9. Nezafat R et al, MRM 2006; 55:858-864
10. Absil J et al, Proc. ISMRM 2007;p.12